EFFECTS OF PREHEATING AND INTERPASS TEMPERATURE ON STRESSES IN S 1100 QL MULTI-PASS BUTT-WELDS

P. Wongpanya [a1] Th. Boellinghaus [a2] G. Lothongkum [b] Th. Kannengiesser [a3]

[a] Federal Institute for Materials Research and Testing (BAM) (Germany)
[b] Department of Metallurgical Engineering, Chulalongkorn University (Thailand)
E-mail: [a1] pornwasa.wongpanya@bam.de, [a2] thomas.boellinghaus@bam.de, [a3] thomas.kannengiesser@bam.de, [b] gobboon.l@chula.ac.th

ABSTRACT

Most of the research on Hydrogen Assisted Cold Cracking (HACC) in high strength steel welds conducted over the last several decades has focused on single-pass welds, especially considering materials with yield strengths about 700 MPa. The guidelines for avoiding cracking that have been developed from such work are therefore useful only where a root pass is the critical event. The well-known guideline is using preheating temperature. Such guideline is very limited when applied to multi-pass welds. In order to support this need, this paper presents the influence of inhomogeneous Hydrogen Removal Heat Treatment (HRHT) procedures, i.e. sole preheating, controlled interpass temperature and combined preheating and controlled interpass temperature, on the residual stresses in multi-pass welds of S 1100 QL. Thereafter, these results are used to identify HACC problems in S 1100 QL and are not reported here. The results were achieved by decent thermal and structural finite element simulations of a five-layer welded 12 mm thick plate at a realistic restraint provided by respective Instrumented Restraint Cracking (IRC) test. The simulations show that the inhomogeneous heat treatment procedures significantly increase the residual stresses as compared to welding without any heat treatment. In contrast to more general anticipations, an increasing controlled interpass temperature does not necessarily lead to a stress reduction, but can even increase the stresses dependent on the location in the multi-pass welds. Maximum residual stresses generally appear in the upper third part of the weld and are not located beneath the top surface where is a typical location used to detect residual stresses in real welded components. If the restraint intensity given to the welded component is not proper, such heat treatment procedures with various temperatures seem to be useful to reduce residual stresses in multi-pass welds.

IIW-Thesaurus keywords: *Cold cracking; Cracking; Defects; Heat treatment; High strength steels; Mathematical models; Multirun welding; Preheating; Residual stresses; Restraint; Steels; Structural steels; Temperature; Weldability tests.*

1 INTRODUCTION

Up to the present, preheating and a controlled interpass temperature represent the most frequently applied to decrease the cold crack sensitivity of high strength structural steel welds. As one effect of preheating, raising of the cooling time $t_{8/5}$ and consequently, softer microstructures were considered in the past. Additionally, it is anticipated that preheating provides longer times after welding at higher temperatures and thus, promotes a faster hydrogen transport due to higher diffusivities. For this, quite a number of various procedures using nomograms, equations and algorithms based on carbon equivalents were developed in the past to evaluate appropriate pre-

Doc. IIW-1851-07 (ex-doc. IX-2240r1-07) recommended for publication by Commission IX “Behaviour of metals subjected to welding”.

heating temperatures. However, such procedures cannot be applied to modern high strength structural steels, like the S 1100 QL steel investigated here. As another reason for such failures appears the fact that the test procedures used for the respective standards and specifications usually do not reflect appropriately the restraint intensity and inhomogeneous heat treatment given to real welded components. Regarding real components, it has also to be considered that high strength structural steels are usually applied for respective weight reduction, often resulting in heavily stiffened constructions [1], [2]. In other words, the multi-pass welds of such steels are usually subjected to high restraints producing high stresses and strains. As outlined in previous contributions [3], [4] three parts of joints have to be considered for the total restraint (Figure 1). This means that the weld edge preparation ($R_{Fy,1}$), the plate or pipe dimensions ($R_{Fy,2}$) and the surrounding construction ($R_{Fy,3}$) contribute individually to the intensity of restraint and thus, these three parts have to be evaluated to calculate the total restraint intensity ($R_{Fy,total}$) of a welded structure by

$$\frac{1}{R_{Fy,total}} = \frac{1}{R_{Fy,1}} + \frac{1}{R_{Fy,2}} + \frac{1}{R_{Fy,3}} \quad (1)$$

The shrinkage restraint transversely to a real weld is usually determined ahead of welding and simply represents the spring constant of the material surrounding the joint. It can thus be evaluated by the transverse reaction force F_y related to the respective root gap displacement in both transverse directions $2\cdot\Delta y$, normalized by the total weld length l_w:

$$R_{Fy} = \frac{F_y}{2\,\Delta y \cdot l_w} \quad (2)$$

In contrast to laboratory investigations under restrained-weld, previous results [6] clearly showed that sole preheating causes higher local residual stresses (at the HAZ adjacent to the fusion line) in root welds than without any heat treatment. Moreover, from the three dimensional plot in Figure 2 it becomes clear that increasing the preheating temperature even increases the transverse residual stresses more than increasing the restraint intensities from the conditions of restraint-free to rigid clamping. It is also remarkable that the transverse residual stresses are more increased at preheating temperatures of up to 150 °C than at higher temperatures ranging between 150 °C and 300 °C, which is usually avoided to prevent annealing effects and a loss in strength. To summarize this, preheating of S 1100 QL root welds at lower temperature produces a significant stress increase at practical welding applications and thus, is at least pointless for cold cracking avoidance.

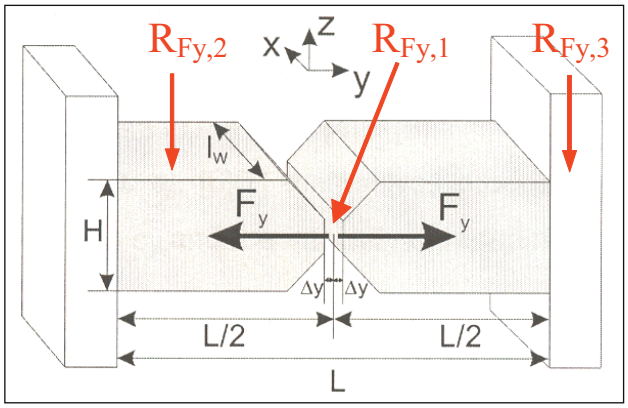

Figure 1 – Schematic illustration relating to the definition of the restraint intensity $R_{Fy,total}$ [5]

As a further step towards clarifying the welding requirements for these steels, restrained and non-restrained multi-pass welds have been investigated in this study with respect to the effects of Hydrogen Removal Heat Treatment (HRHT) procedures on the residual stresses by means of numerical analysis.

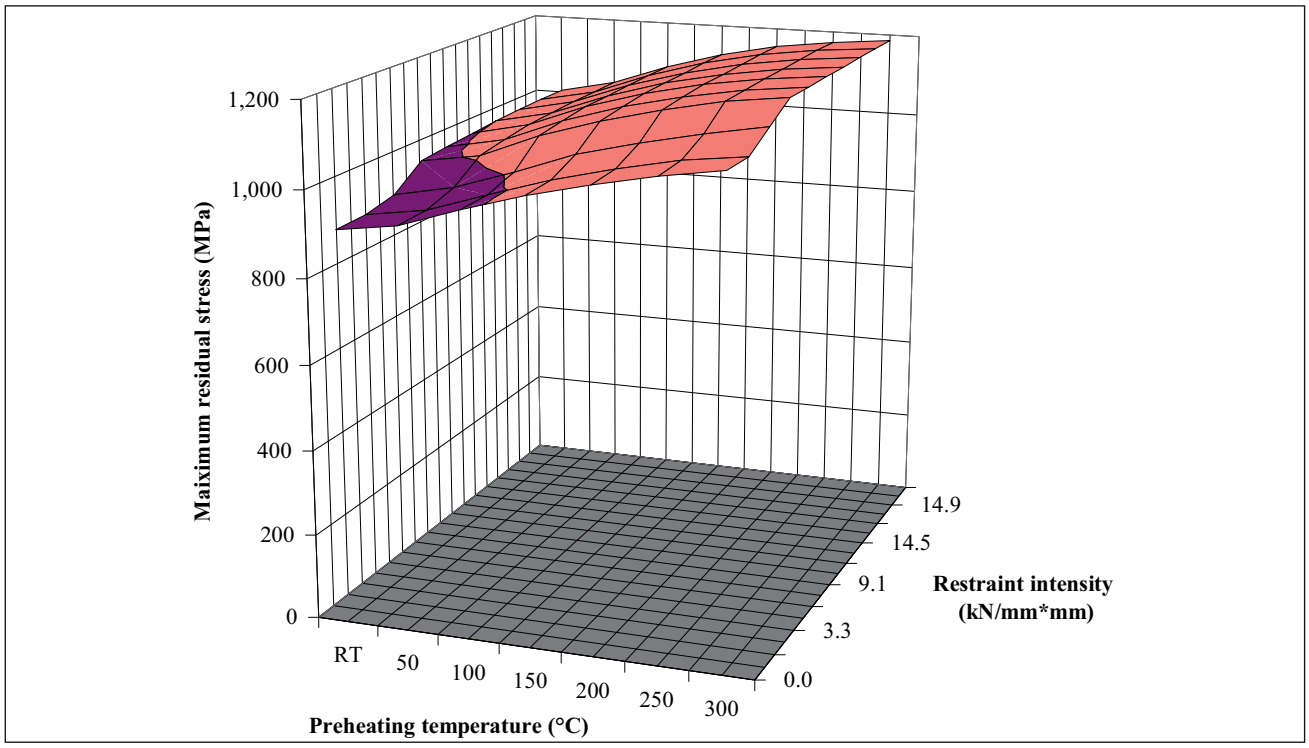

Figure 2 – Calculated Stress-Restraint-Heating (SRH) diagram for the root layer of S 1100 QL [6]

2 EXPERIMENTAL AND NUMERICAL PROCEDURES

2.1 Experimental procedure

For both, the experiments as well as the numerical analyses, the fine-grained structural steel S 1100 QL is considered as a base material. The chemical compositions of the base material and the filler wire are summarized in Table 1. In order to take account of practical application and of the fact that a matching commercial filler material for the steel S 1100 QL is not yet available; welding is carried out with a slightly undermatching filler wire (Union X96). Thus, the strength level in the weld metal and the heat-affected zone (HAZ) is slightly lower than that in the base material and exhibited lowest yield strength of 985 MPa, as shown by the mechanical properties of hydrogen-free S 1100 QL and Union X96 in Table 2. The Instrumented Restraint Cracking (IRC) test plates are GMA welded using a multi-pass welding method and a plate thickness of H = 12 mm, a weld length of l_w = 100 mm, a total restraint length of L = 110 mm as well as the parameters presented in Table 3 for each sequence.

The stiffness of the IRC-Frame, in which the welding tests were executed, was measured to be C_{Frame} = 1.35 kN/µm by applying a specific force to the frame using a hydraulic cylinder and measuring the resulting expansion between the clamping devices. Using Equation (2) and considering the usual weld length of l_w = 100 mm of the IRC-Specimens the intensity of restraint provided by the IRC-Frame is 13.5 kN/(mm·mm). However, this restraint intensity only represents the structural stiffness of the surrounding assembly parts, i.e. $R_{Fy,3}$ [see Equation (1)]. The total restraint intensity considering a restraint length of the plates of L/2 = 55 mm on each side of the weld, a plate thickness of H = 12 mm and the applied V-bevel butt was 15.05 kN/(mm·mm), as calculated by respective linear-elastic finite element analysis.

Table 1 – Chemical compositions of the base and filler material (wt.-%)

Materials	C	Si	Mn	Cr	Mo	Ni
S 1100	0.17	0.27	0.85	0.46	0.45	1.88
Union X96	0.12	0.78	1.86	0.46	0.53	2.36

Table 2 – Mechanical properties of hydrogen-free S 1100 QL weld microstructures [7]

Mechanical properties	S 1100 QL			WM Union X96
	BM	CHAZ	FHAZ	
Tensile strength [MPa]	1 348	1 366	1 399	1 071
Yield strength [MPa]	1 150	1 000	1 010	985
Rupture strain [%]	15	15	15	14
Reduction of area [%]	69	64	65	51

2.2 Numerical procedures

To determine the residual stresses in the multi-pass welds of S 1100 QL, decoupled thermal and structural two dimensional analyses are carried out by using commercial finite element program with code name ANSYS. In such procedures, the nodal results of the non-linear transient thermal calculations are used as body force for the subsequent non-linear structural elastic-plastic numerical analysis. For the preceding thermal finite element analyses, the thermo-physical properties which can affect the finally calculated stresses and strains are very carefully selected from Richter's diagrams [8] for steel having a chemical composition similar to the relatively new S 1100 QL type. The temperature dependent values of the density, heat convection coefficient, specific heat and thermal conductivity are shown in Figures 3 a) and 3b) and are applied to all microstructures in the respective

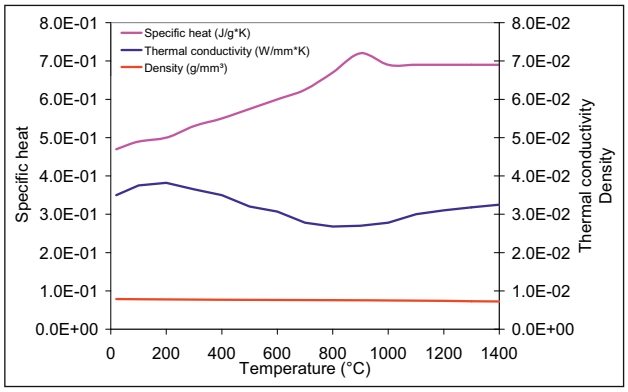

a) Density, thermal conductivity and specific heat

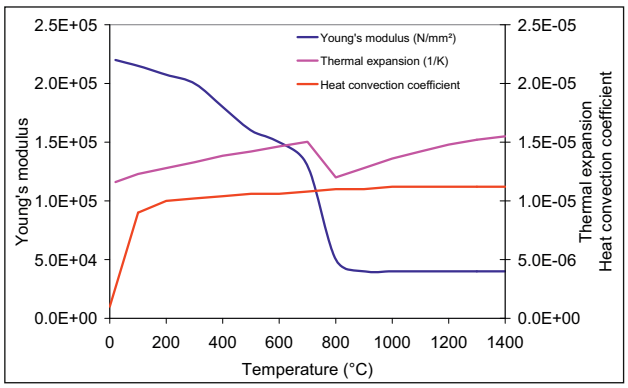

b) Thermal expansion, heat convection coefficient and Young's modulus

Figure 3 – Temperature dependent thermo-physical properties for transient thermal analyses [8]

Table 3 – Welding conditions for each pass

Pass number	Welding current (A)	Arc voltage (V)	Wire speed (cm/min)	Preheating and interpass temperature (°C)
1	290	32.5	50	25-30
2	300	32.4	50	30-30
3	300	32.4	50	30-30
4	300	32.4	50	30-30
5	300	32.4	50	30-30

analyses. Generally, the thermo-mechanical properties vary with the weld microstructure. For instance, the yield strength and the ultimate tensile strength change drastically, if steel is austenitized during heating or the austenite decomposes into a martensitic-bainitic microstructure during cooling. As another point, the percentage of martensite produced between martensite start and finish temperature follows a complex function. The true stress-strain behaviour is determined experimentally for the various simulated weld microstructures and is shown in Figure 4. For simplification, the complex microstructure transformation processes were modelled by respective interpolation between the various temperature dependent stress-strain curves (Figure 4) and by the temperature dependent thermal expansion coefficient [Figure 3 b)]. For simulation of the heating process during welding, the nodes of each layer are set to a homogeneous temperature above the melting point (≤ 1 540 °C) of the steel for three seconds including an ascending time of one second simulating travelling of a torch through the respective cross section. After welding, cooling by heat convection and by heat conduction is simulated by application of surface film coefficients at all free surfaces of the model. Subsequently, the same welding conditions as for the first layer have been simulated for the next four layers. Cooling of the second and the fourth layers have been simulated down to the respective interpass temperature as summarized in Table 4. All simulations are carried out for cooling of the final weld to room temperature.

Consistently with the respective IRC test, the location of the weld microstructures and the welding sequences are shown in Figures 5 a) and 5b), respectively. Also the effect of another welding sequence as shown in Figure 5 c) has been investigated. Reheating of the previous weld beads has been considered by the thermo-mechanical properties in the above described way.

Since only a marginal part of the load can be carried by the austenitic as compared to the martensitic-bainitic microstructure and the present study is targeted to show the principal effects of heat treatment temperatures which are far lower than the effects of transformation temperatures of the investigated steel types on the respective stresses, these simplifications are regarded as tolerable. As a much more important point, the influence of the restraint intensity on the reaction stresses has been considered in the numerical simulations, i.e. the effect of rigid clamping resulting in a considerably high restraint intensity of R_{Fy} = 15.2 kN/(mm·mm) has been compared to low restraint intensity at a value of R_{Fy} = 0.1 kN/(mm.mm) which has been simulated by respective elements with a

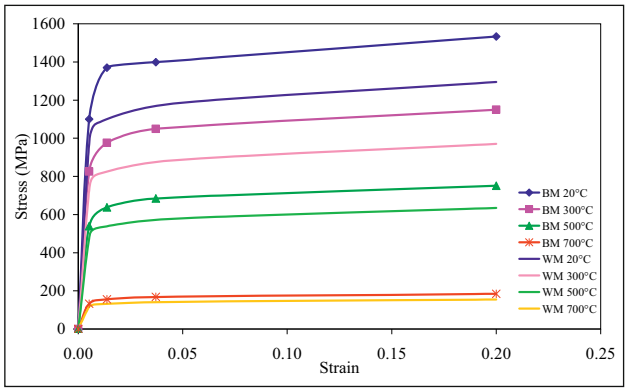

a) Modified values for the base metal and the weld metal

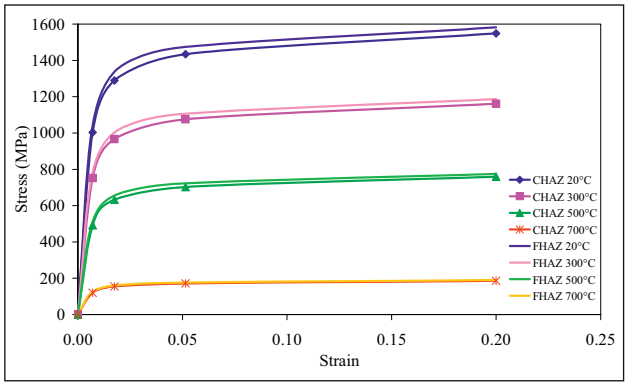

b) Modified values for the coarse grain heat-affected zone and the fine grain heat-affected zone [7]

Figure 4 – True stress-strain behaviour of S 1100 QL steel as thermo-mechanical properties for structural analysis

very small spring constant to avoid rigid body movements in the simulations [Figure 5 d)]. Previous studies [4] showed that regarding the dependence of the residual stresses on the restraint intensities and the different weld microstructures it has to be distinguished between the near field and the far field of the weld. For these reasons, the effect of the restraint intensities as well as of the heat treatment temperatures on residual stresses has been investigated in the HAZ adjacent to the fusion line (local residual stresses) and at the end of the weld (reaction stresses). In order to simulate the heat dissipation into the clamping devices of the IRC-test facility or similarly, into a surrounding construction, a constant temperature has been assigned to both ends of the model. Heat convection has been modelled at all free surfaces of the weld. As described previously and as confirmed by respective pre-analyses, heat loss by radiation can be neglected for solid materials in contrast to liquids and has thus been ignored in the modelling procedure.

Table 4 – Heat treatment conditions for multi-pass welds

Temperature (°C)				
Experiment	FEM			
	Without any heat treatment	Sole preheating temperature	Controlled interpass temperatures	Combined preheating and controlled interpass temperatures
RT-RT	RT-RT	120-RT	RT6120	120-120
		180-RT	RT-180	180-180
		250-RT	RT-250	250-250

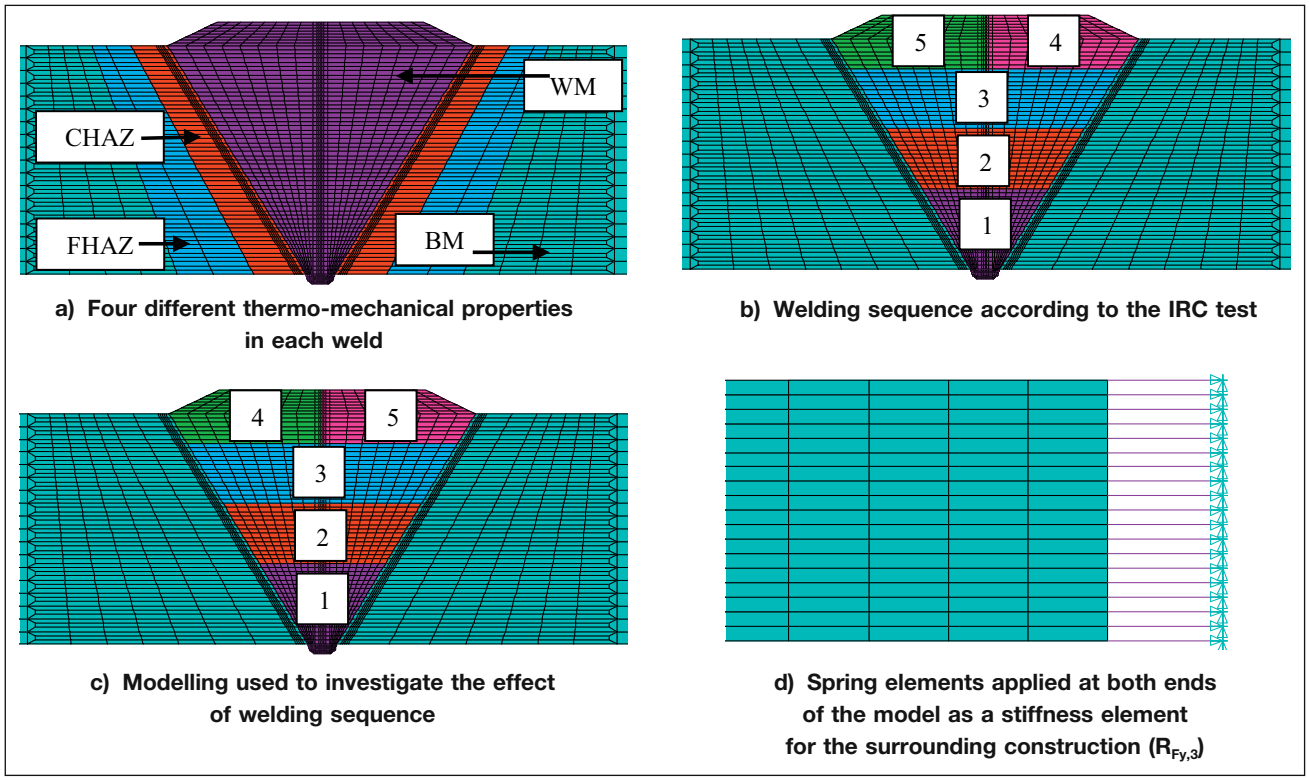

a) Four different thermo-mechanical properties in each weld

b) Welding sequence according to the IRC test

c) Modelling used to investigate the effect of welding sequence

d) Spring elements applied at both ends of the model as a stiffness element for the surrounding construction ($R_{Fy,3}$)

Figure 5 – Boundary conditions of simulation

The heat treatment temperatures have been calculated based on the carbon equivalent [9] and ranged between 120 °C and 250 °C as shown in Table 4 which are sufficiently low to avoid any detrimental strength reduction and microstructure changes in S 1100 QL steel. Usually, preheating of such weld is carried out by heating pads, which have been modelled by assignment of the respective temperatures to those nodes on the surface where heating pads are located for the specific times. For applying the interpass temperature to the simulations of the multi-pass welds, the lump elements of the next layer were added to the mesh periodically after the previous layer was completed and cooled down to the specific interpass temperature. For the simulation of combined preheating and controlled interpass temperature respective macro files and subroutines have been written to steer the commercial finite element program.

3 RESULTS AND DISCUSSION

3.1 Comparison of numerically and experimentally evaluated thermal cycles

In order to get a better reliability of FEM results, the cooling time between 800 °C and 500 °C, $\Delta t_{8/5}$, is listed in Table 5 for various heat treatment procedures, i.e. sole preheating (120 °C-RT), controlled interpass (RT-120 °C) and combined preheating and controlled interpass temperatures (120 °C-120 °C). The values rely on temperature measurements at the third layer, i.e. at half of the weld metal height, and are compared to the respective numerically determined values at the same location in the model. The numerically calculated cooling time $\Delta t_{8/5}$ without heat treatment temperatures (RT-RT) is slightly faster than that of the experiment. The

Table 5 – Comparison of different calculated cooling times with respect to the preheat and interpass temperature

Cooling time 800 °C/500 °C (second)				
Experiment	FEM			
RT-RT	RT-RT	120 °C-RT	RT-120 °C	120 °C-120 °C
12	11	11	15	15

small deviation of one second might be caused by different temperature fields as a consequence of small simplifications in the model regarding the actual weld bead shape and size.

As shown by Figure 6, the experimentally and numerically obtained temperature histories at the surface of the IRC-test plates at a distance of 25 mm from the centre line of the weld are fairly well consistent. At temperatures below 100 °C, a slightly higher calculated cooling rate can

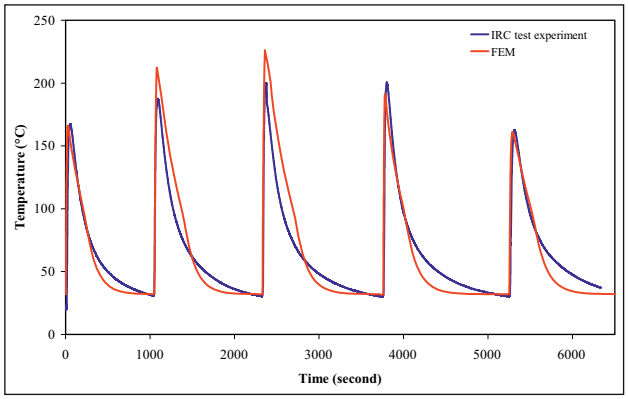

Figure 6 – Simulated and measured temperature histories at the specific point in a distance of 25 mm from the weld centreline with the preheating and interpass conditions of RT-RT

be observed which may be related to the boundary condition, i.e. the constant temperature at both ends of the model. However, no phase transformation takes place in this temperature range, and it can thus be anticipated that the faster cooling rate does not significantly influence the thermo-mechanical behaviour. As expected, with increasing preheating and interpass temperatures also respectively longer cooling times have been calculated (Table 5). It has already been shown earlier [6] at root welds that if the thermal cycles coincide well between experiment and simulation also the structural analyses were comparable to the experiments, i.e. they revealed nearly the same stress and strain levels. The purpose of this investigation by numerical simulation is to show the principal effects of preheating and interpass temperature on the weld residual stresses. This means that the total agreement of the stresses and strains between experiments and numerical simulations is of lower priority for the present study. For this reason, the residual stresses have not been measured during the experiments and have not been compared to the calculated values in this study.

3.2 General shape of the transverse residual stress distribution

To show the distribution of the transverse residual stresses in the weld, nodes at several locations were depicted in the transverse direction of the weld and for various heights, i.e. at the top of the layers one to three, as indicated by L01, L02, L03, respectively, and 0.70 and 1 mm underneath the top surface, as indicated by 0.7 and 1.0, respectively. In the following diagrams, such values have been assigned versus the distance across the welded component. Transverse residual stresses in the weld are shown without application of heat treatment procedures for restrained-weld [Figure 7 a)] and for restraint-free weld [Figure 7 b)], respectively.

Under restrained-weld, it becomes clearly that the residual stresses in the near (local stress) and in the far field (reaction stress) of the weld are significantly increased with the heights of welded structure. In the near field, the highest residual stresses of about 900 MPa are located in the upper part of the third layer at the HAZ adjacent

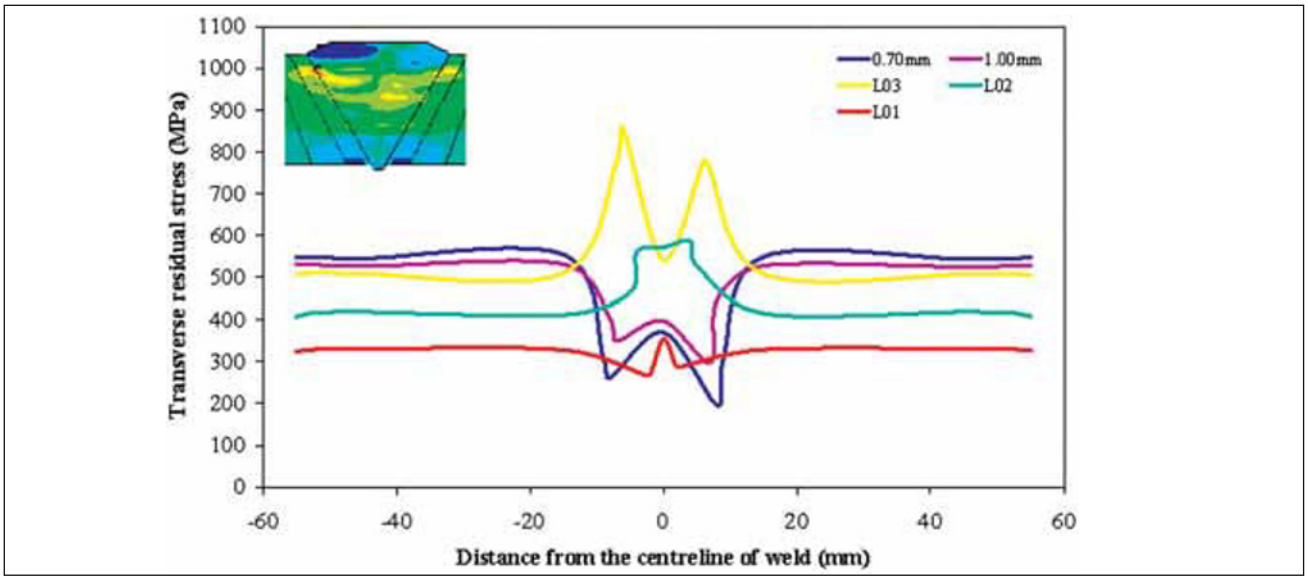

a) High restraint (15.2 kN/mm·mm)

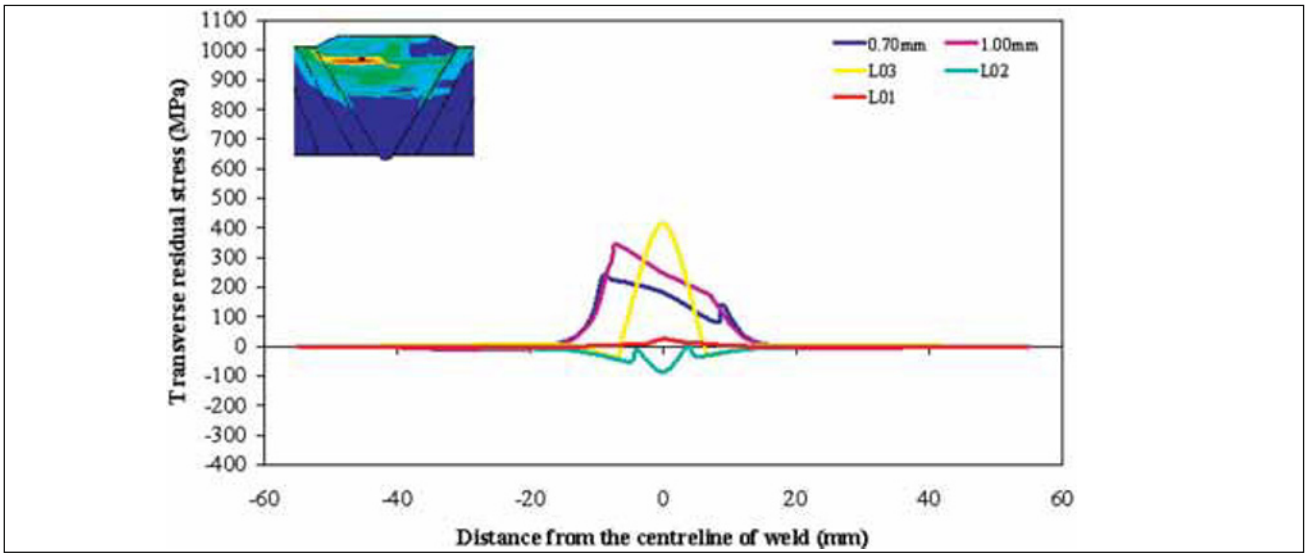

b) Low restraint (0.1 kN/mm·mm)

Figure 7 – Transverse residual stress distribution after cooling down to room temperature for one day at different total restraint intensities ($R_{Fy,total}$)

to the fusion line. In the far field, the maximum residual stresses of about 580 MPa appear 0.70 mm underneath the top surface. The lowest reaction stresses have been registered in the root weld with a value of about 360 MPa. Differences between the top side and the bottom part of the weld might also be attributed to suppress bending of the weld by rigid clamping.

At restraint-free weld, no reaction stresses are observed. The local residual stresses in the weld are not only larger, but have also quite a different shape, if subjected to an external restraint. However, the maximum residual stresses can still be observed in the third layer, but are shifted from the fusion to the weld centreline and range only at about 400 MPa.

3.3 Effects of sole preheating temperature on residual stress distribution

The transverse residual stress distribution is markedly influenced by the application of sole preheating temperature of 120 °C, as shown by Figure 8.

At the restrained weld, sole preheating shifts both, the local residual stresses in the weld region and the reaction stresses in the far field towards higher values. From a comparison of Figure 7 a) to Figure 8 a), it becomes obvious that the residual stresses in the root weld (curves L01) are significantly affected by sole preheating. For instance, the residual stresses at the root weld are increased to about 600 MPa and also above the level of the top side. Still, the maximum residual stresses appear at the fusion line of the third layer. In the far field, the reaction stresses at the bottom part of the weld are also increased by sole preheating. However, at the top side of the weld, the effect of sole preheating is not pronounced, i.e. the reaction stress level remains nearly the same. For practical applications, this means that sole preheating affects the final reaction stress level predominantly at the root side of the weld where probably most of the additional thermal strains resulting from inhomogeneous preheating have to be taken up.

At the restraint-free weld, sole preheating causes lower residual stresses at the top side and also in the root weld

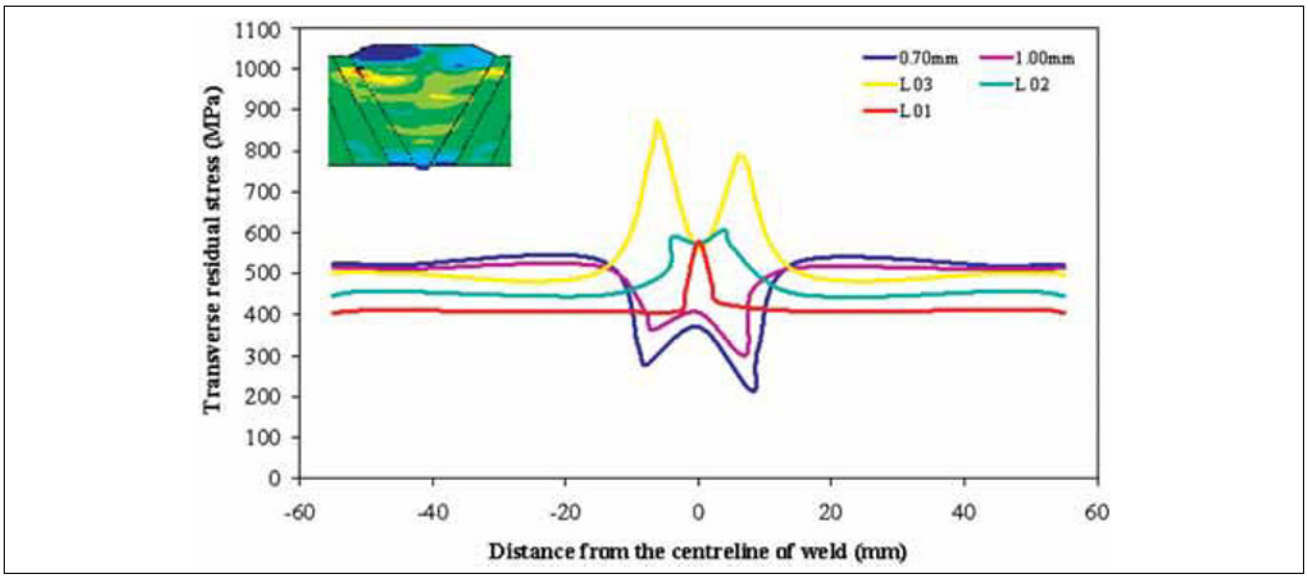

a) High restraint (15.2 kN/mm·mm)

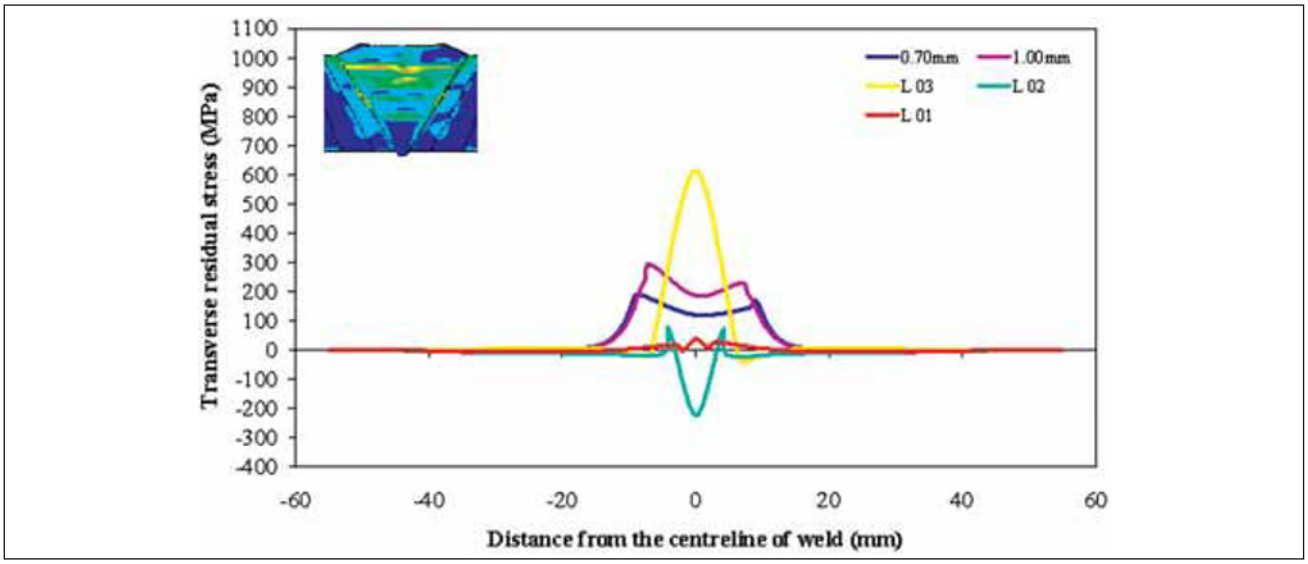

b) Low restraint (0.1 kN/mm·mm)

Figure 8 – Effects of sole preheating temperature of 120 °C on transverse residual stress distribution after cooling down to room temperature for one day at the different total restraint intensities ($R_{Fy,total}$)

region. In comparison to the non-heat treated weld [Figure 7 b)], sole preheating at 120 °C reduced the local residual stresses 1.00 mm underneath the top surface from nearly 400 MPa to about 300 MPa [see Figure 8 b)]. However, the maximum local residual stresses still appear in the region of the third layer (curves L03) and are increased from about 400 MPa [Figure7 b)] to about 600 MPa by sole preheating at 120 °C [see Figure 8 b)].

3.4 Effects of controlled interpass temperature on residual stress distribution

As represented by Figure 9, the transverse residual stress distributions are influenced by welding with controlled interpass temperature of 120 °C.

At the restrained weld, it becomes clear from a comparison of Figure 7 a) to Figure 9 a) that increasing controlled interpass temperature significantly increases the transverse residual stress level. This applies to both, the local stresses in the near field of the weld and the reaction stresses in the far field. For example, the maximum local residual stresses still appear at the fusion line of the third layer and are increased from about 900 MPa [Figure7 a)] to above 900 MPa when controlled interpass temperatures of 120 °C, is applied. Only at the location of the root weld (curve L01), the local residual stresses are reduced to about 200 MPa. The reaction stresses at the upper part of the weld are significantly increased by the controlled interpass temperature. For instance, the residual stress 0.70 mm underneath the top surface is increased from about 600 MPa [Figure7 a)] up to 680 MPa. More general and for practical welding, these results show that under restrained-weld, the local stresses and the reaction stresses of the weld are increased by about 100 MPa, if controlled interpass temperature is applied instead of welding with cooling of each layer down to room temperature.

At the restraint-free weld, welding with controlled interpass temperature of 120 °C generally does not seem to influence the stress level, or even might reduce it in the region of the second run [curve L02, Figure 9 b)].

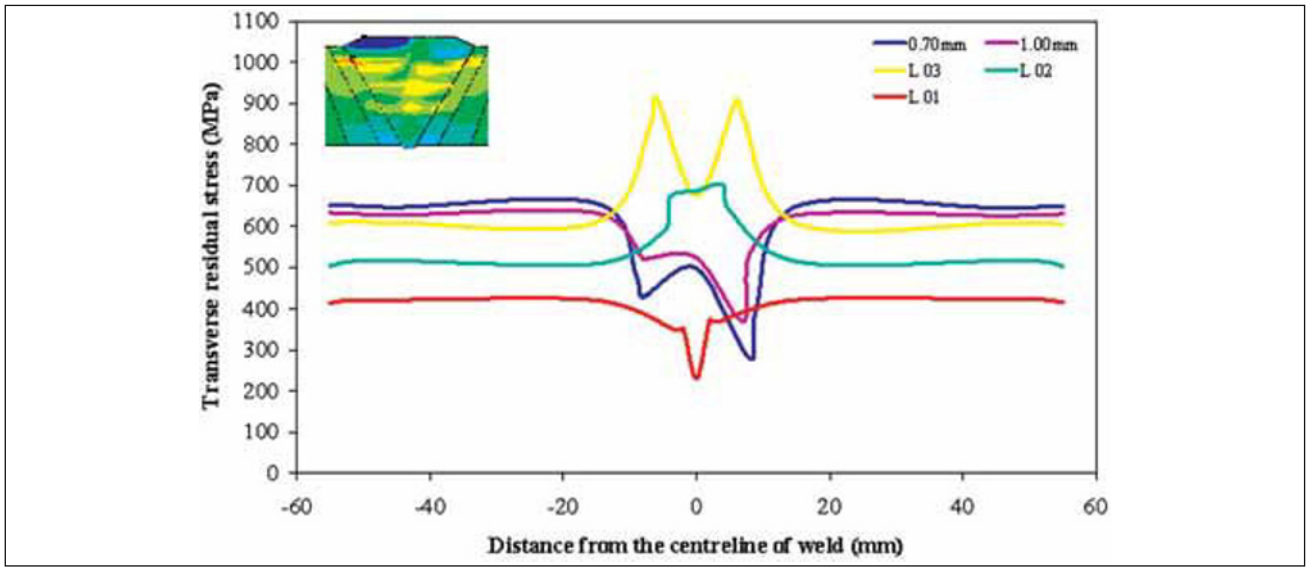

a) High restraint (15.2 kN/mm·mm)

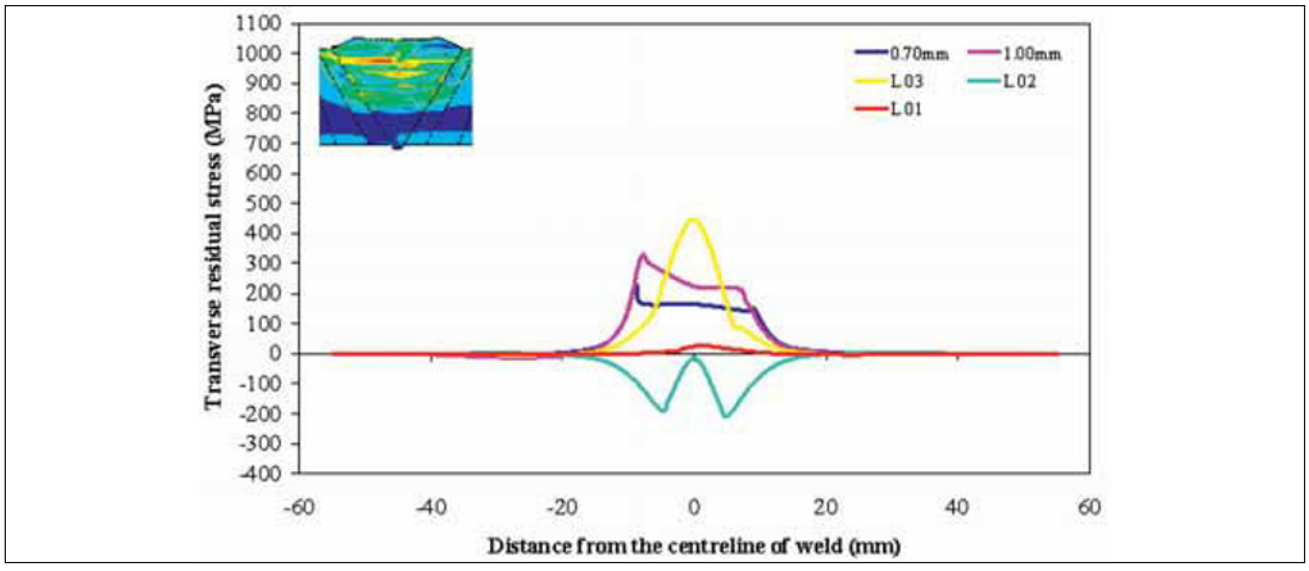

b) Low restraint (0.1 kN/ mm·mm)

Figure 9 – Effects of controlled interpass temperature of 120 °C on transverse residual stress distribution after cooling down to room temperature for one day at the different total restraint intensities ($R_{Fy,total}$)

3.5 Effects of combined preheating and controlled interpass temperature on residual stress distribution

The combined effects of preheating and interpass temperature on the transverse stress distribution have also been investigated and their extreme influence is shown in Figure 10 for combined preheating and controlled interpass temperatures of 120 °C.

At the restrained weld, from a comparison of Figure 7a) to Figure 10 a), it becomes obvious that the local residual stresses 0.70 mm and 1.0 mm underneath the top surface are slightly increased due to such combined heat treatment at temperatures of 120 °C. For instance, the maximum residual stresses 0.70 mm underneath of the top surface are increased from about 600 MPa [Figure 7a)] to up to 680 MPa for 120 °C. At these locations, the effects of the combined heat treatment on the maximum residual stresses [Figure 10 a)] are the same as those arising from sole application of controlled interpass temperature [Figure 9 a)]. However, the local residual stresses in the region of the first three layers of the weld (curves L01, L02 and L03) are significantly increased, if higher temperatures for the combined heat treatment are applied. For example, the maximum local residual stresses at the weld centreline of the first and second layers (curves L01 and L02) are significantly increased from about 360 MPa [Figure 7 a)] up to about 720 MPa [curve L01 in Figure 10 a)] and from about 600 MPa up to 750 MPa [curve L02 in Figure 10 a)] when a combined preheating and controlled interpass temperature of 120 °C is applied.

At the restraint-free weld, by comparison of the local residual stresses in Figure 7 b) and Figure 10 b), it becomes obvious that the local residual stresses 0.7 mm and 1.0 mm underneath the top surface of the weld [Figure 10 b)] are reduced to about half the value, if no heat treatment procedures are applied [Figure 7 b)]. This might be one reason for the fact that combined preheating and controlled interpass temperature is regarded

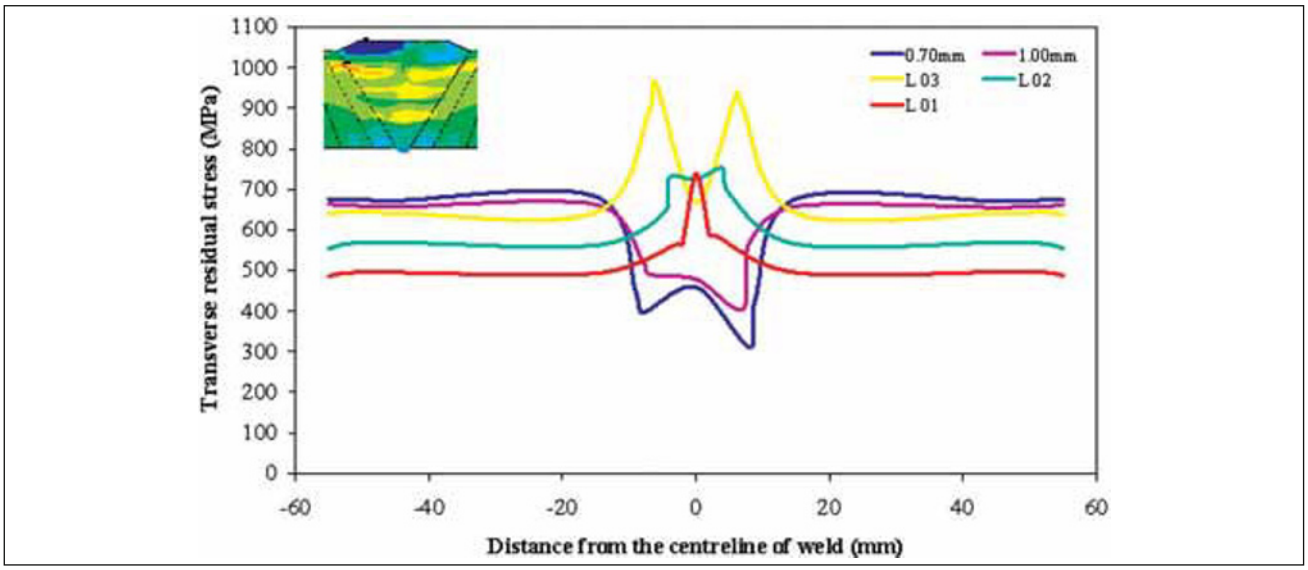

a) High restraint (15.2 kN/mm·mm)

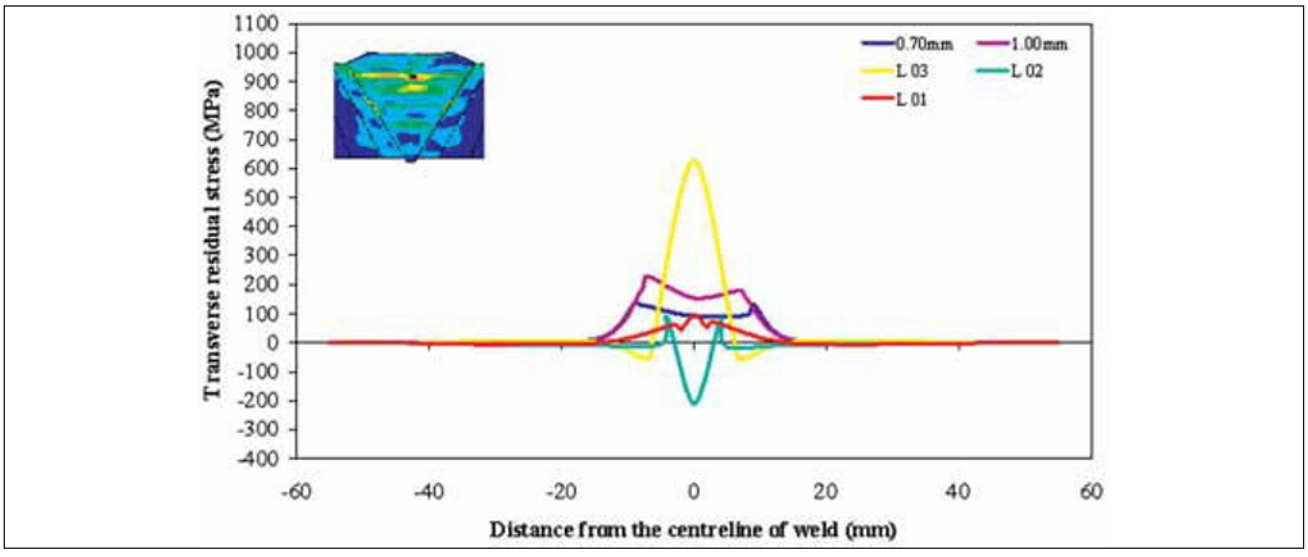

b) Low restraint (0.1 kN/mm·mm)

Figure 10 – Effects of combined preheating and controlled interpass temperature of 120 °C on transverse residual stress distribution after cooling down to room temperature for one day at the different total restraint intensities ($R_{Fy,total}$)

as very beneficial to practical welding. But, it has to be realized that such effect is only limited to the top side of the weld. For instance, the stresses in the region of the third layer (curves L03) are nearly doubled, if a combined heat treatment at a temperature of 120 °C is applied [Figure 10 b)] instead of welding without any temperature control [Figure 7 b)].

In order to better understand heat treatment procedural effects, the maximum residual stresses observed at the fusion line of the third layer and the residual stresses practically measured at the top surface in the near field of the welded component are shown in Figure 11 and Figure 12, respectively.

Figure 11 represents the maximum residual stress located in the upper part of the multi-pass welds in particular, in the HAZ adjacent to the fusion line of the third layer. It becomes obvious that all heat treatments significantly affect the maximum residual stresses.

At restrained welds, without applying any heat treatment, the maximum residual stresses range at a level of about 850 MPa. When the respective heat treatments are applied, i.e. sole preheating, controlled interpass temperature as well as combined preheating and controlled interpass temperature, the maximum residual stresses significantly increase, in particular at high temperatures. For example, at 250 °C the maximum residual stress value reaches approximately the yield strength value of the material.

At restraint-free welds, the maximum residual stresses also increase when the temperatures of 120 °C and 180 °C are applied at sole preheating and controlled interpass temperature. But, they significantly decrease, if higher combined preheating and controlled interpass temperatures are used.

For instance, the maximum residual stresses are reduced to half of their previous level (from 400 MPa to

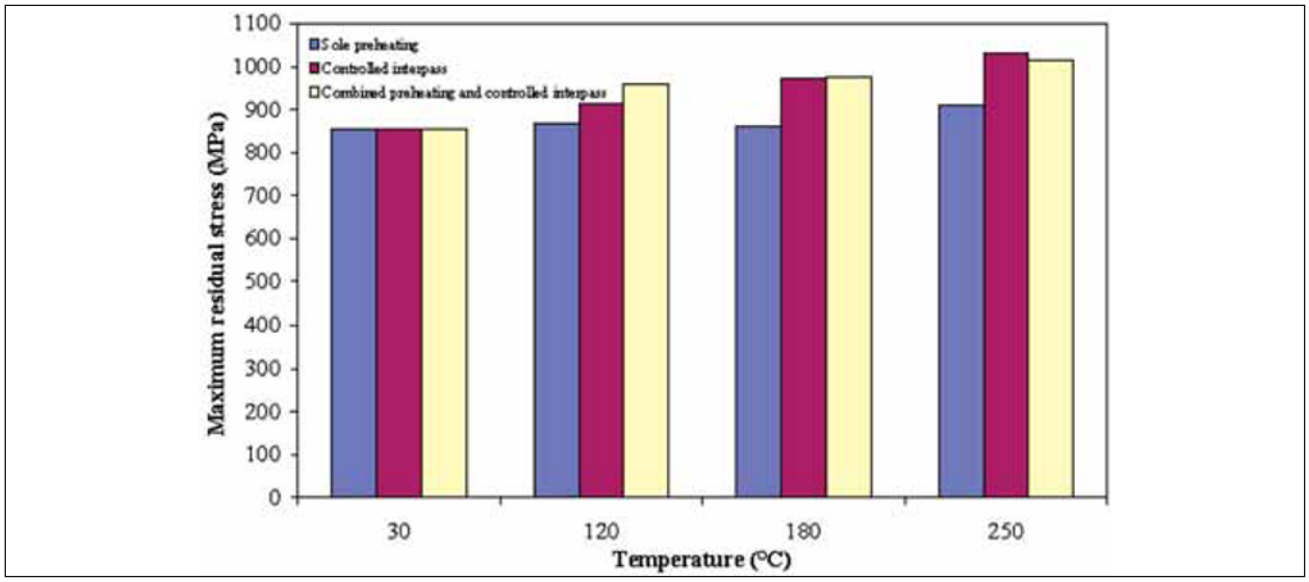

a) High restraint (15.2 kN/mm·mm)

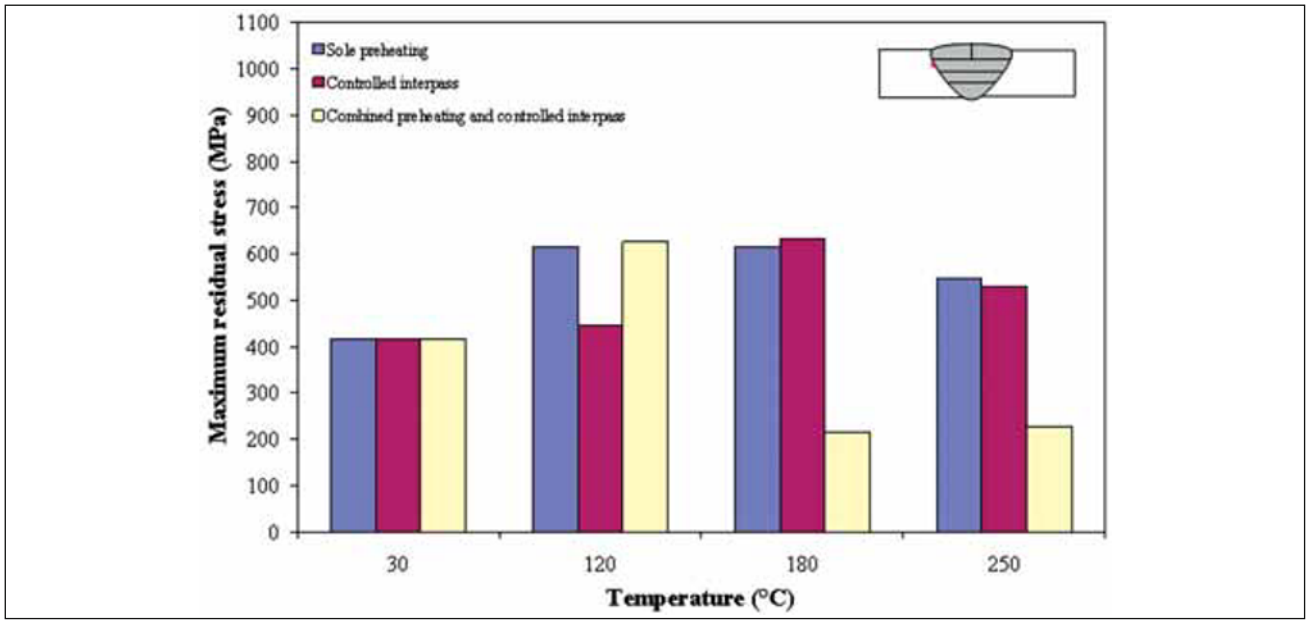

b) Low restraint (0.1 kN/mm·mm)

Figure 11 – Effects of heat treatment procedures on the maximum residual stresses (observed at the fusion line of the third layer) of multi-pass welds in S 1100 QL at the different total restraint intensities ($_{RFy,total}$)

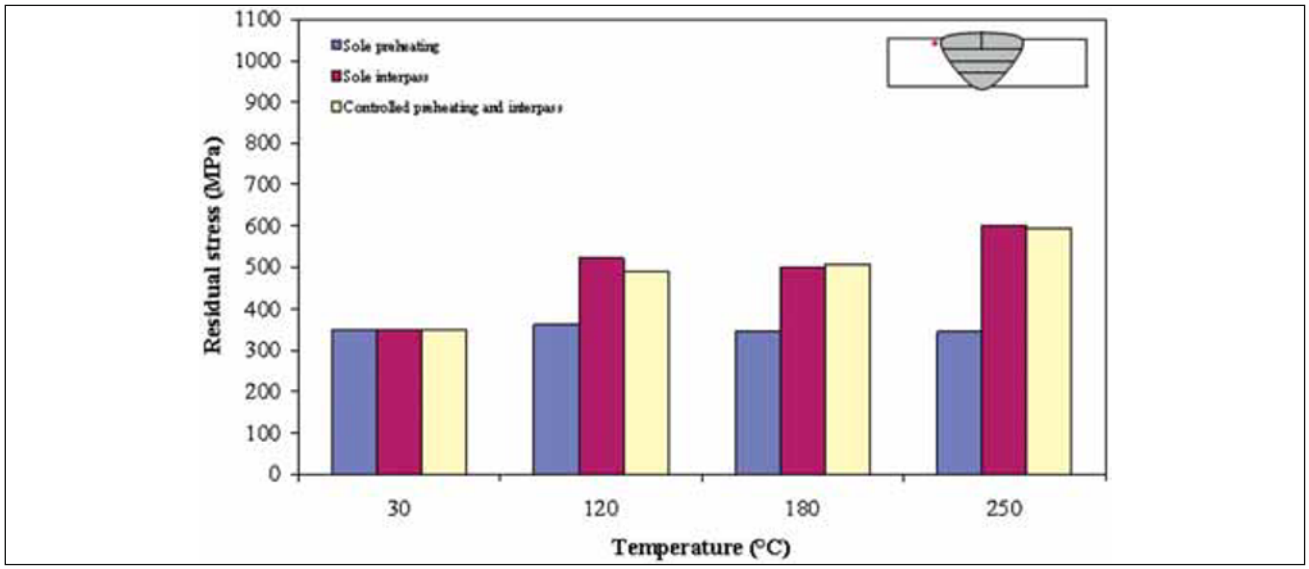

a) High restraint (15.2 kN/mm·mm)

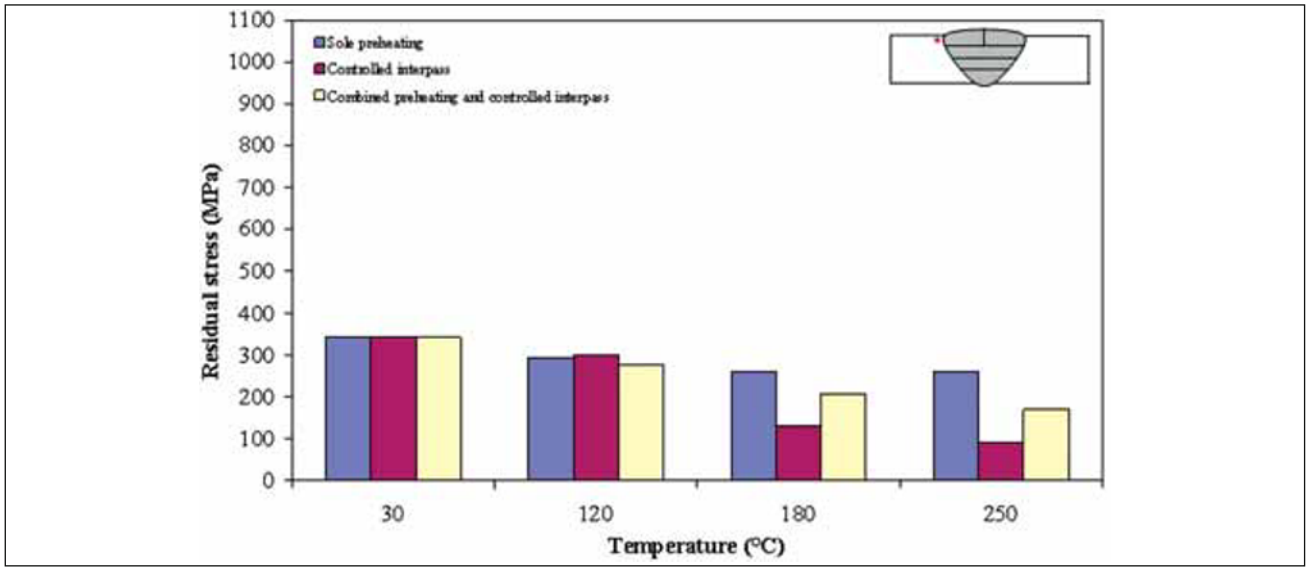

b) Low restraint (0.1 kN/mm·mm)

Figure 12 – Effects of heat treatment procedures on the residual stresses (practically measured at the top surface in the near field of welded component) of multi-pass welds in S 1100 QL at the different total restraint intensities ($R_{Fy,total}$)

200 MPa) at temperatures of 180 °C and 250 °C for the combined heat treatment.

Figure 12 represents the calculated residual stresses practically measured with the help of a blind hole drilled to a depth of about 1.00 mm from the top surface in the near field of the weld.

At the restrained welds, sole preheating does not show any effect on the residual stress level, even if the high temperatures are applied. However, it is clear that the residual stresses continuously increase with temperature, if controlled interpass temperatures and/or combined preheating and controlled interpass temperatures are used in the multi-pass welding process. The residual stress level might reach up to double the value (from 350 MPa to 620 MPa), if a controlled interpass temperature and/or a combined preheating and controlled interpass temperature of 250 °C is applied.

At the restraint-free welds, all heat treatment procedures seem to be very useful in reducing the residual stresses as shown in Figure 12 b). For example, the residual stresses continuously decrease from 350 MPa to about 90 MPa, if a sole interpass temperature of 250 °C is used. However, it has again to be emphasized that free shrinkage represents a very seldom exception during practical fabrication welding.

3.6 Stresses arising during welding depending on preheating and interpass temperature

The above (Figure 1 to Figure 12) described results were obtained from practical measurement of the local residual stresses and reaction stresses in the near and far field after completion of welding and cooling of the weld down to room temperature. However, it is generally expected that the stresses arising during welding and before welding the subsequent layer can be reduced by increasing the preheating and the interpass temperature. In order to better understand these effects, the

stresses arising within the time of welding the individual layers, i.e. the so-called interpass stresses, are assigned to Figure 13 to Figure 15 after the first, second and third layer for heat treatment combinations at temperatures of up to 120 °C. As the most realistic case, this investigation was carried out only for the completely externally restrained welds. Figure 13 to Figure 15 shows exemplarily the interpass-stress distributions transverse to the welding direction after cooling down to a specific temperature. For instance, the 120-120 condition means that a preheating and controlled interpass temperature of 120 °C has been applied. The RT-RT condition means that no preheating and no controlled interpass temperature have been selected. After welding of the first layer and cooling to room temperature, the interpass stresses are depicted transversely to the weld specimen beneath the top surface. After the first layer has cooled down to 120 °C, the interpass stresses are measured at the same positions.

From all three diagrams (Figure 13 to Figure 15) it becomes obvious that preheating drastically increases the stress level between welding of each layer. For example, after welding of the first layer the maximum interpass stresses are shifted from about 980 MPa to about 1 080 MPa in the near field and from about 180 MPa to above 300 MPa in the far field, if sole preheating is applied for 30 minutes at 120 °C. In contrast, the interpass stresses are significantly reduced, if an interpass temperature of only 120 °C is applied. It has to be noticed that the interpass stresses after welding of the second and the third layer are much less affected by the heat treatment procedure (Figure 13 to Figure 15) and thus, all of such heat treatment procedures have the greatest effects on the stresses between welding of the first and the second layer.

4 CONCLUSIONS

Considering the effects of heat treatment procedures, i.e. sole preheating, controlled interpass as well as combined preheating and controlled interpass temperature,

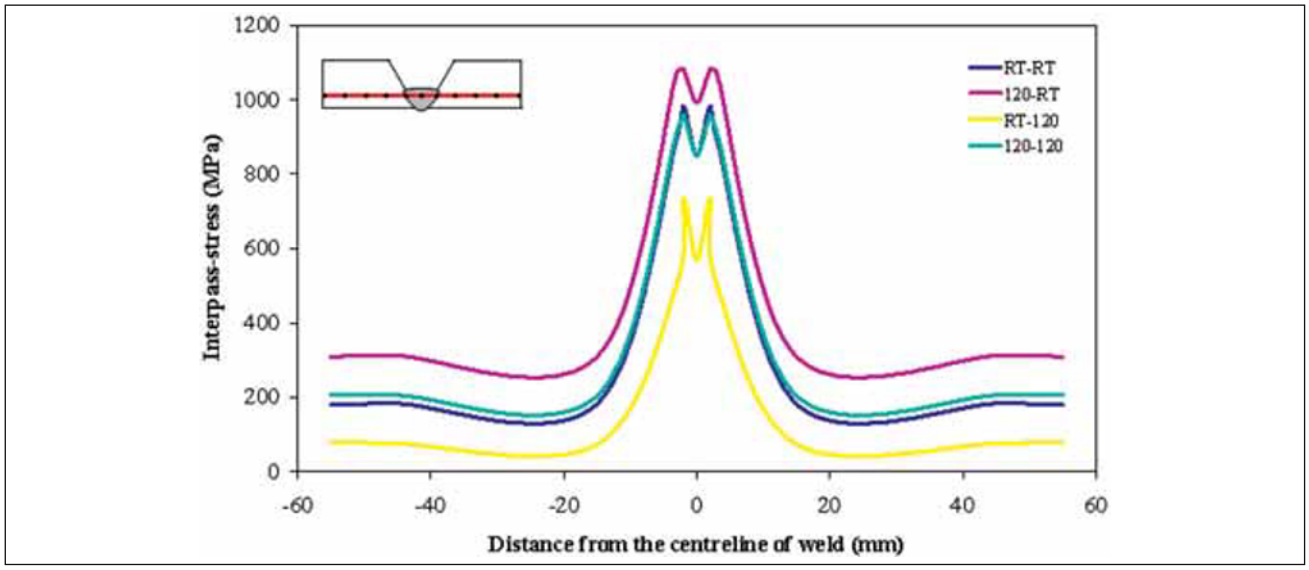

Figure 13 – Transverse interpass-stress distributions of the 1st layer after completion of welding at the specific conditions

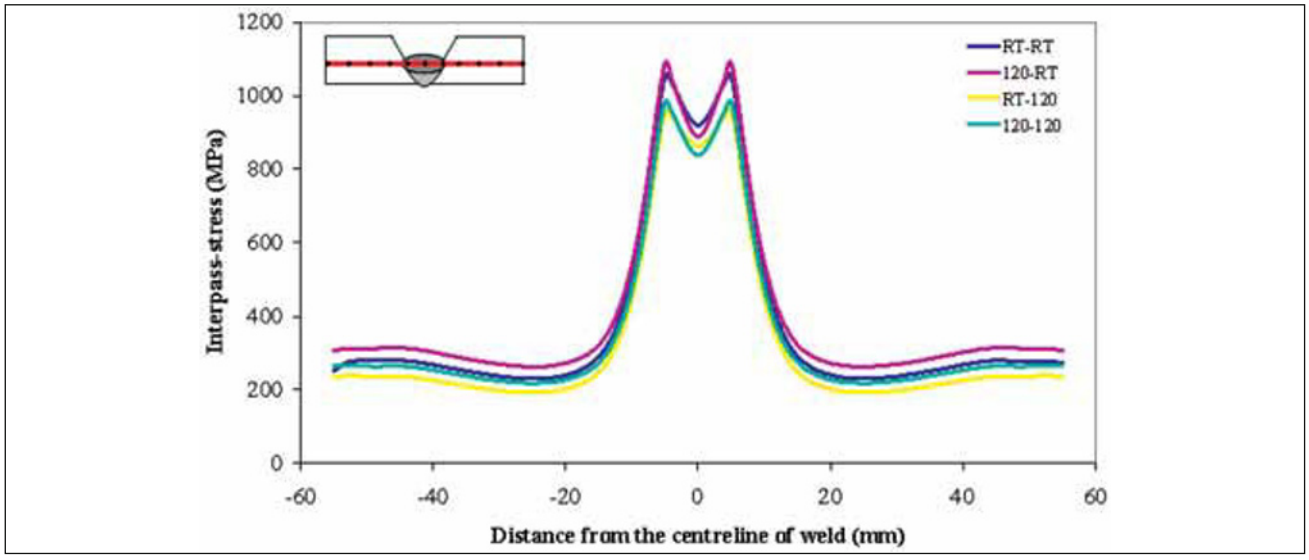

Figure 14 – Transverse interpass-stress distributions of the 2nd layer after completion of welding at the specific conditions

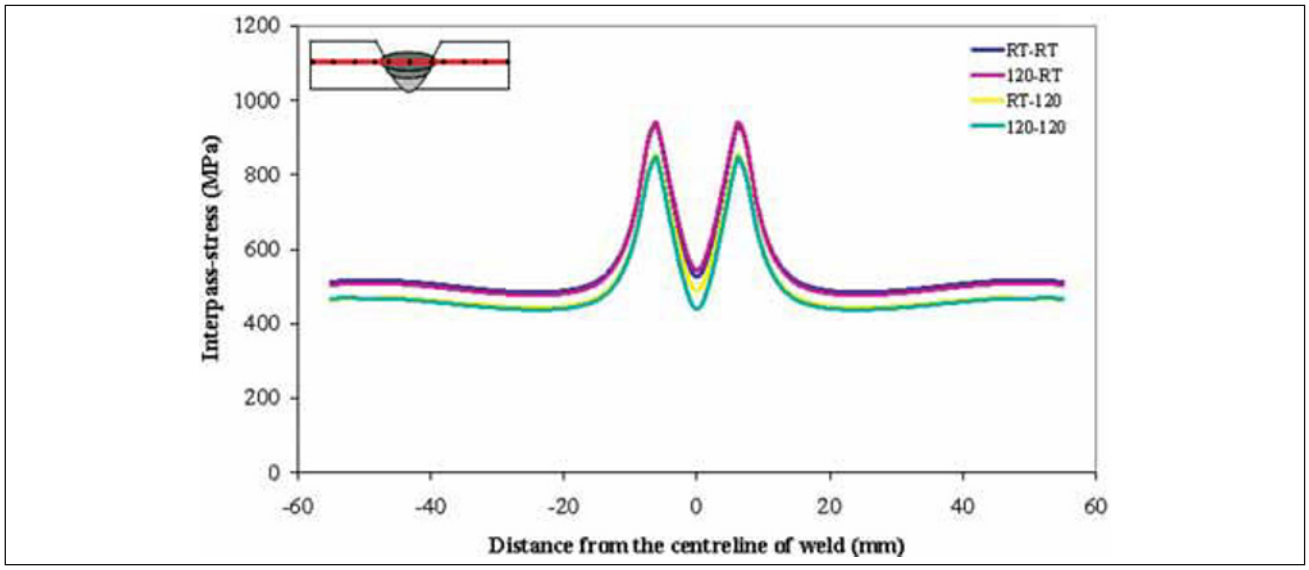

Figure 15 – Transverse interpass-stress distributions of the 3rd layer after completion of welding at the specific conditions

on stresses in S 1100 QL multi-pass welds, the following conclusions can be drawn:

1. Application of all heat treatment procedures generally increases the local residual stresses and the reaction stresses after welding and cooling to room temperature of the restrained weld.

2. As expected, no reaction stresses evolve in restraint-free weld. The local residual stresses after welding and cooling of the restraint-free weld to room temperature might be reduced at the top side of the weld by respective heat treatment procedures.

3. For the interpass-stresses, application of sole preheating also increases the stresses between welding of the various layers, if no controlled interpass temperature is applied, i.e. if the weld cools down to room temperature between the layers. A controlled interpass temperature significantly reduces the stresses after welding of the root layer, if the welds are not preheated ahead of welding. However, these effects are less pronounced during welding of the later layers towards completion of the weld. If preheating is applied, the stresses evolving between welding of the layers can only be reduced by additional application of a controlled interpass temperature to that level which is achieved without any heat treatment.

4. As already shown by Graville [10], in multi-pass welds the location of the highest residual stresses is dependent on the location of the last filling layer. This also means that the residual stress distribution transverse to the weld is not symmetrical, if two layers are applied at the top side. This effect is found when the welding sequence of the fourth and the fifth layers is exchanged [see Figures 5 c) and d)], so that the fifth layer is altered to the right side, and the highest residual stress position is shifted from left to right remaining at the fusion line of the third layer. However, the reaction stresses in the far field are not affected by such procedure.

5. For practical applications, it is necessary to consider the restraint intensity given to the welded components. If the restraint intensity is not appropriate, all heat treatment procedures in multi-pass welding seem to be very useful to decrease the stress level in the welded components. This might lead to misunderstanding of the effects of heat treatment procedures on residual distributions in high strength structural steel welds.

6. The sensitivity of residual stresses to sole preheating temperatures is less significant in multi-pass welds than in root welds (see Figure 11 and Figure 12). This means that the criteria applied to root welds cannot be used for multi-pass applications, even if all welding parameters are the same.

7. With respect to HACC avoidance in multi-pass high strength structural steel welds further investigations by numerical analysis have to show whether or not heat treatment procedures contribute to a reduction of hydrogen concentration.

REFERENCES

[1] Hever M., Schröter F.: Modern steel-high performance material for high performance bridges, 5th International Symposium on Steel Bridges, March 2003, Barcelona, pp. 80-91.

[2] Hanus F., Schröter F., Schütz W.: State of art in the production and use of high-strength heavy plates for hydropower applications, Proc. Conf. on High Strength Steels for Hydropower Plants, Graz, 2005, paper 13.

[3] Mayer B., Nolde P., Diers G., Sarhil Y., Rosert R.: Entwicklung neuer und Optimierung vorhandener MSG-Fülldrähte für das Schweiβen hochfester Feinkornstähle, DVS-Bericht 225, 2003, pp. 443-451.

[4] Boellinghaus Th., Kannengiesser Th., Neuhaus M.: Effects of the structural restraint intensity on the stress strain build up in butt joints, Mathematical Modelling of Weld Phenomena 7, H. Cerjak ed., Technical University Graz, pp. 651-670.

[5] Boellinghaus Th., Hoffmeister H., Ruyter E.: Calculation of restraint intensities by finite element analysis for the assessment of weldability, H. Cerjak *et al.* (ed), Mathematical Modeling of Weld Phenomena 3, London, 1997, pp. 606-623.

[6] Wongpanya P., Boellinghaus Th., Lothongkum G.: Effects of hydrogen removal heat treatment on residual stresses in high strength structural steel welds, Welding in the World, 2006, Volume 50, Special Issue, pp. 96-130.

[7] Zimmer P., Boellinghaus Th., Kannengiesser Th.: Effects of hydrogen on weld microstructure mechanical properties of the high strength structural steels S 690 Q and S 1100 QL, IIW doc. II-A-141-04\II-1525-04.

[8] Richter F.: Die wichtigsten physikalischen Eigenschaften von 52 Eisenwerkstoffen, Heft 8, Verlag Stahleisen, Düsseldorf.

[9] Florian W.: Cold cracking in high strength steel weld metal: Possibilities to calculate the necessary preheating temperature, IIW doc. IX-2006-01.

[10] Graville B.A.: Interpreventive report on the weldability tests for hydrogen cracking of higher strength steels and their potential for standardization, Welding Research Council Bulletin 400, 1995, pp. 1-44.

COMPOGRAVURE, IMPRESSION, BROCHAGE
IMPRIMERIE CHIRAT, 42540 ST-JUST-LA-PENDUE
MARS 2008, DÉPÔT LÉGAL 2008 N° 8744
NUMÉRO D'INSCRIPTION À LA COMMISSION PARITAIRE : EN COURS.